Journal of Hazardous Materials 414 (2021) 125471

Contents lists available at ScienceDirect

Journal of Hazardous Materials

journal homepage: www.elsevier.com/locate/jhazmat

Ex vivo exposure to different types of graphene-based nanomaterials consistently alters human blood secretome

Sandra Ballesteros [a], Josefa Domenech [a], Antonia Velázquez [a,b], Ricard Marcos [a,b,*], Alba Hernández [a,b,*]

[a] Group of Mutagenesis, Department of Genetics and Microbiology, Universitat Autònoma de Barcelona, Spain
[b] Consortium for Biomedical Research in Epidemiology and Public Health (CIBERESP), Carlos III Institute of Health, Madrid, Spain

ARTICLE INFO

Editor: Dr. S. Nan

Keywords:
Graphene-based-nanomaterials
Blood secretome
Ex vivo exposure
Cytokines
Inflammation

ABSTRACT

The biomedical applications of graphene-based nanomaterials (GBN) have significantly grown in the last years. Many of these applications suppose their intravenous exposure and, in this way, GBN could encounter blood cells triggering an immunological response of unknown effects. Consequently, understanding the relationships between GBN and the immune system response should be a prerequisite for its adequate use in biomedicine. In the present study, we have conducted a little explored *ex vivo* exposure method in order to study the complexity of the secretome given by the interactions between GBN and blood cells. Blood samples from different healthy donors were exposed to three different types of GBN widely used in the biomedical field. In this sense, graphene oxide (GO), graphene nanoplatelets (GNPs), graphene nanoribbons (GNRs) and a panel of 105 proteins representatives of the blood secretome were evaluated. The results show broad changes in both the cytokines number and the expression levels, with important changes in inflammatory response markers. Furthermore, the indirect soft-agar assay was used as a tool to unravel the global functional impact of the found secretome changes. Our results indicate that the GBN-induced altered secretome can modify the natural anchorage-independent growth capacity of HeLa cells, used as a model. As a conclusion, this study describes an innovative approach to study the potential harmful effects of GBN, providing relevant data to be considered in the biomedical context when GBN are planned to be used in patients.

1. Introduction

Nanomaterials have caught the attention of the scientific community due to their unique physicochemical properties and multiple applications. To date, there is a growing literature about the potential biomedical applications of different nanomaterials in fields such as bioimaging, transplants, drug delivery, and diagnosis (Ramos et al., 2017).

In the case of graphene-based nanomaterials (GBN), they have shown a significant potential for biomedical applications, including gene therapy, drug delivery, tumor therapy, and theragnostic (Han et al., 2019; Song et al., 2020). Additionally, graphene has been widely used as a contrast agent in magnetic resonance imaging due to its magnetic properties (Lin et al., 2016; Loh et al., 2018). To date, the applications of graphene oxide are receiving more attention than other GBN such as graphene nanoplatelets (GNPs) or graphene nanoribbons (GNRs) that are still in a more preclinical phase.

Although GBN applications look promising, one limitation to reach clinical practice is that after its intravenous administration, GBN meet blood cells, potentially inducing immune perturbations (Boraschi et al., 2018; Fadeel, 2019). Thus, previous works have reported differential impacts of different forms of graphene oxide on primary human immune cell populations (Orecchioni et al., 2016, 2017). This has also been observed in the case of other nanomaterials. Hence, it is known that aluminum oxide nanoparticles induced an altered immune response in mice when intravenously injected (Park et al., 2016). Likewise, long-term exposures (up to 60 days) to subtoxic doses of palladium nanoparticles *via* intravenous injection alter the cytokine serum levels in treated Wistar rats, suggesting a possible impact of these nanoparticles on the immune system after long-term exposures (Iavicoli et al., 2018).

Different studies have been conducted to determine the potentially harmful effects of GBN exposure, as recently reviewed (Madannejad

* Corresponding authors at: Group of Mutagenesis, Department of Genetics and Microbiology, Universitat Autònoma de Barcelona, Edifici Cn, Campus de Bellaterra, Cerdanyola del Vallès, 08193 Barcelona, Spain.
E-mail addresses: ricard.marcos@uab.cat (R. Marcos), alba.hernandez@uab.cat (A. Hernández).

https://doi.org/10.1016/j.jhazmat.2021.125471
Received 23 July 2020; Received in revised form 16 January 2021; Accepted 17 February 2021
Available online 20 February 2021

et al., 2019). The reported results are heterogeneous depending on different factors including the used model (*in vitro vs in vivo*), and the evaluated target, among others. It is true that the results obtained using *in vivo* studies permit an easier extrapolation for human risk assessment; nevertheless, such studies have inconveniences such as the cost and the associated ethical considerations. In this scenario, it has been proposed that *ex vivo* exposure using human blood represents a better model to evaluate the biological interactions of nanomaterials than the use of *in vitro* studies involving mammalian cell lines (Cui et al., 2015). In fact, it has been proved that polyethylene glycol nanoparticles have a different response when evaluated *in vitro* with 3T3 fibroblast and C1R lymphoblast cells, than when tested using whole blood as a more complex system. Another advantage of using this human model is that the inclusion of different donors–with different genetic backgrounds-can highlight key differences depending on the donor patient (Mann et al., 2016).

According to the above indicated, we have carried out a systematic study involving the analysis of the effects of the three GBN mainly used in biomedicine (GO, GNPs, and GNRs) after incubation in fresh whole blood samples obtained from different donors. Changes in the blood cells secretome were analyzed, since it is known that it can reflect a potential health problem (da Cunha et al., 2019). The analyzed proteins included hormones, cytokines, chemokines, interferons, colony-stimulating factors (CSFs), growth factors, tumor necrosis factors (TNFs), and other bioactive molecules. All of them are biomarkers of pathophysiological processes such as cell differentiation, invasion, metastasis, autophagy, apoptosis, tissue organization, immune surveillance, angiogenesis, and cell-to-cell communication in cancer cells (Patel et al., 2014). Furthermore, and to understand whether the induced secretome alterations entail further functional implications, an indirect version of the soft-agar was also performed (Annangi et al., 2015; Vila et al., 2017).

2. Materials and methods

2.1. Nanomaterials characterization

GO, GNPs and GNRs were all obtained from Sigma-Aldrich (St. Louis, USA). Transmission electron microscopy (TEM) was used to determine both the size and the morphology of the selected GBN on a JEOL JEM-1400 instrument (Jeol LTD, Tokyo, Japan). Likewise, the characterization of both hydrodynamic size and zeta potential of the three selected GBN were determined, after dispersion in 0.05% bovine serum albumin (BSA), by using dynamic light scattering (DLS) and laser Doppler velocimetry (LDV) methodologies, respectively. Such measurements were performed on a Malvern Zetasizer Nano-ZS zen3600 instrument. Layered graphene materials, GO and GNPs, were further characterized to determine its thickness in a mechanical Profiler 7.0 P15 (KLA Tencor, California, USA) with a stylus radius of 2 μm and an applied force of 2 mg. For this metrological characterization, stock solutions of graphene nanomaterials were diluted to 50 μg/mL in miliQ water and air-dried on a silicon substrate. 20 randomly selected GO or GNPs particles were scanned at 20 μm/s, to determine their thickness.

2.2. Whole blood exposure to graphene-based nanomaterials

According to the Nanogenotox protocol (Nanogenotox, 2011), GO (2 mg/mL) and GNPs (1 mg/mL) were dispersed in 1% bovine serum albumin (BSA) in MilliQ water. The nanomaterials in the dispersion medium were sonicated for 16 min and a 10% amplitude sonication to obtain a final concentration of 1.9 and 0.95 mg/mL, respectively. GNRs were prewetted in 0.5% absolute ethanol and dispersed in 0.05% bovine serum albumin (BSA) in MilliQ water. As before, GNRs in the dispersed medium were sonicated for 16 min and a 10% amplitude sonication, to obtain a final concentration of 2.56 mg/mL.

Fresh human whole blood was extracted from 8 healthy donors (4 males and 4 females, between 25 and 45 years old) and stabilized with EDTA (1%). From each donor, 4 mL of blood were exposed to a final non-cytotoxic concentration of 50 μg/mL of each type of GBN, lipopolysaccharides (LPS from *Escherichia coli* O55:B5; Sigma-Aldrich (Saint Louis, USA)) at 4 μg/mL (positive control), and equal amounts of vehicle (negative control) for 24 h at 37 °C, and constant agitation at 80 rpm to avoid sedimentation. After the incubation, blood was centrifuged at 1600*g* during 10 min to obtain the serum.

2.3. Determination of cytokine expression changes

The Human XL cytokine Array Kit (R&D Systems Bio-techne, Proteome Profiler™) was used to determine changes in the cytokine's expression induced by each GBN. Cytokine membranes were incubated with 350 μL of serum overnight at 4 °C and constant agitation at 100 rpm and then, manufacturer's instructions were followed. Briefly, serum samples were diluted and mixed with a cocktail of biotinylated detection antibodies. This mixture was then incubated with the array. The array included membranes spotted in duplicate with capture antibodies. Any cytokine/detection antibody complex present was bound by its cognate immobilized capture antibody on the membrane. Streptavidin-horseradish peroxidase and chemiluminescent detection reagents were added, and a signal was produced in proportion to the amount of cytokine bound. Then, membranes were visualized using the GeneGnome XRQ enhanced chemiluminescence system (ECL, Cell Signaling Technologies, Danvers, MA). Finally, relative quantification of cytokine expression was assessed using the ImageJ Protein Array (Carpentier, 2009). Data were imported to String Database to generate functional cytokines association networks (Szklarczyk et al., 2015).

2.4. Indirect soft-agar

Serum from each donor after treatment with GO, GNPs, GNRs, LPS, or vehicle were used for an indirect soft-agar assay as in Annangi et al. (2015) and Vila et al. (2017) with some modifications. Briefly, HeLa cells used as cell model were collected and filtered through a 40 μm mesh to obtain single-cell suspensions. A suspension of 7×10^4 cells in 1.4 mL of each serum was mixed in a 1:1:1 ratio with 1.2% bacto-agar (DIFCO, MD, USA), and 2X DMEM supplemented with 20% of FBS, 2% NEEA, 2% L-Glu 200 mM and 2% of penicillin-streptomycin. This mixture was enough to prepare triplicates of 2×10^4 cells per well by dispensing 1.5 mL over a 0.6% base-agar (supplemented with 2X DMEM) in each well of a 6-well plate. Plates could sit for 30 min, and then kept in the cell incubator. After 15 days of incubation, plates with cell colonies were stained with 1 mg/mL of INT solution (2-p-iodophenyl-3-p-nitrophenyl-5-phenyl tetrazolium chloride; Sigma, MO, USA). Finally, plates were scanned at high resolution for image analysis using the colony cell counter enumerator software OpenCFU (3.9.0), and the NIST's Integrated Colony Enumerator (NICE) software (NIST, Boulder, CO).

3. Results

3.1. GBN characterization

To complement the information obtained from the supplier, further characterization of the used GBN was carried out. TEM images show the morphology of the selected GBN after sonication (Fig. 1). As shown in Fig. 1A, GO is a single-layered nanomaterial. GNPs are nanoparticles of different sizes and irregular shapes with higher electron density because of their multilayer conformation (Fig. 1A). Finally, GNRs present a graphene fibbers-like shape (Fig. 1A). To better characterize GNRs, information on mean size and SD of the width was calculated by measuring isolated fibers in random fields. The mean ± SD values of GNRs were 118 ± 39 nm (Fig. 1B).

Other measurements such as the hydrodynamic radius and Z-potential for fresh GBN dispersions (100 μg/mL in 0.05% BSA) were

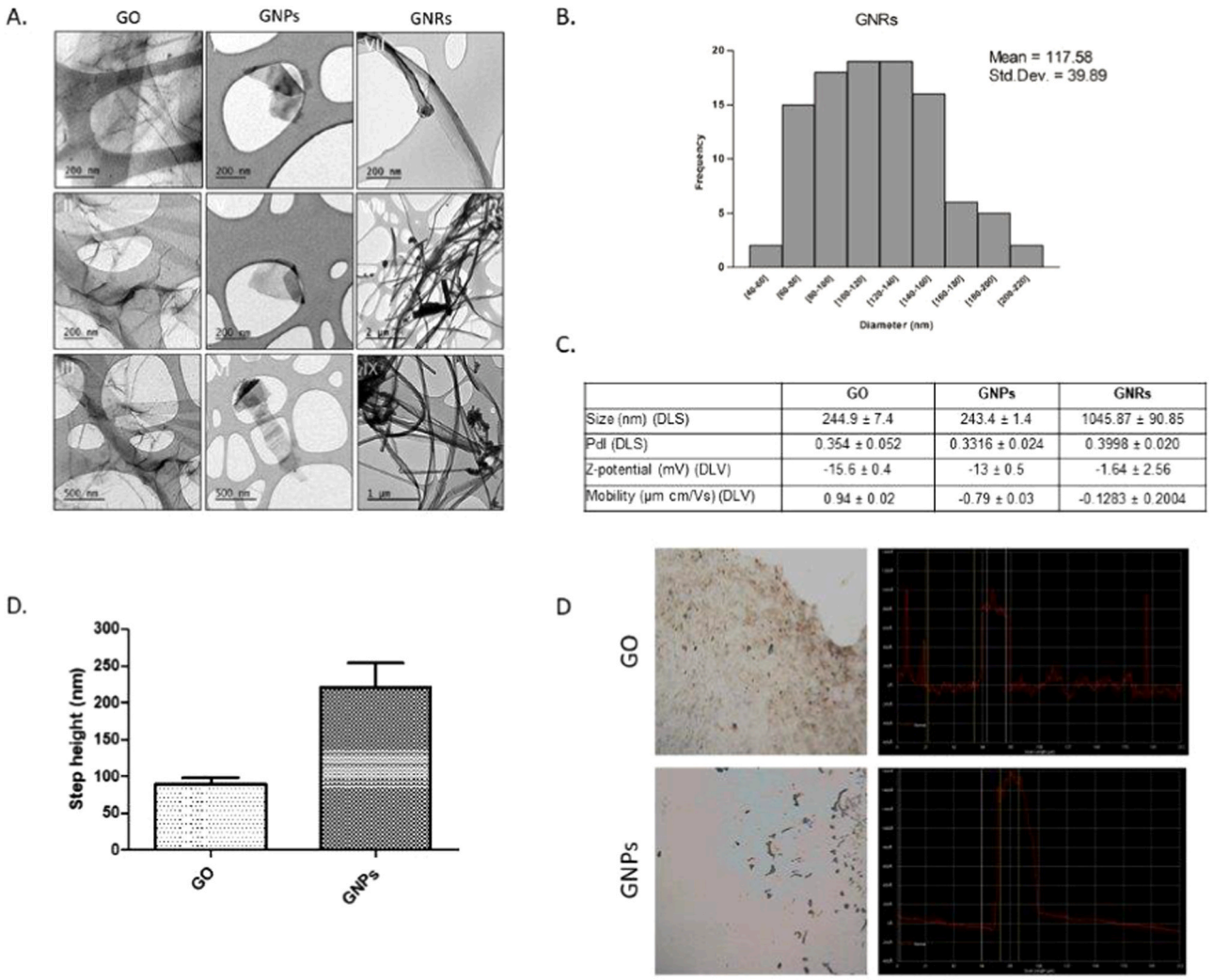

	GO	GNPs	GNRs
Size (nm) (DLS)	244.9 ± 7.4	243.4 ± 1.4	1045.87 ± 90.85
PdI (DLS)	0.354 ± 0.052	0.3316 ± 0.024	0.3998 ± 0.020
Z-potential (mV) (DLV)	-15.6 ± 0.4	-13 ± 0.5	-1.64 ± 2.56
Mobility (μm cm/Vs) (DLV)	0.94 ± 0.02	-0.79 ± 0.03	-0.1283 ± 0.2004

Fig. 1. Characterization of GO, GNPs, and GNRs. (A) TEM representative images of the selected GBN dispersed in water. (B) Size distribution histogram from TEM images of GNRs. (C) GBN average size and charge in distilled water by TEM and DLS. Data are represented as mean ± SD (n = 3). (D and D′) Metrological characterization of GO and GNPs by Profiler 7.0. The analysis of a representative GO and GNPs particle is shown in D′: white arrows indicate the scanner path over the selected GO or GNPs particle and the diagram of the measured profile for GO or GNPs particles is shown. The mean step height measured for GO and GNPs is indicated in the graph D. Data are represented as mean ± SEM (n = 20).

determined (Fig. 1C). Characterization data in the Z-sizer show sizes of 244.9 ± 7.4 nm and 243 ± 1.4 nm for GO and GNPs, respectively. The hydrodynamic radius analysis for GNRs is not a reliable indicator to conclude the size of these nanoparticles since as showing the z-potential value (− 1.64 ± 2.56) they present an important level of aggregation/agglomeration. This value should tend to be around 30 or − 30 mV when there is no aggregation, but in the case of GNRs, it is very close to 0, which indicates aggregation. Furthermore, the obtained polydispersion index (PdI) indicates that dispersions are homogenous since all three values tend to zero (0.354 ± 0.052 for GO, 0.3316 ± 0.024 for GNPs, and 0.3998 ± 0.020 for GNRs). In order to determine the thickness of GO and GNPs, we analyzed the step height using the Profiler 7.0 P15. A mean thickness of 89.42 ± 8.30 nm and 220.26 ± 33.68 nm was determined for GO and GNPs, respectively (Fig. 1D). These results agree with the single- and multi-layer conformation of GO and GNPs nanoparticles and correlate with the TEM observations. Representative measurements for GO and GNPs particles are shown in Fig. 1D′. Data are represented as mean ± SEM.

3.2. Cytokines expression changes

Volcano plots obtained by the R version 3.6.3 (2020-02-29) ggplot2 package are depicted in Fig. 2, showing the 105 cytokines measured after the different GBN treatments, that showed no toxicity (cell viability for 50 μg/mL GO, GNPs and GNRs treatments were 99.1 ± 1.6, 99.4 ± 1.2 and 96.7 ± 4.1, respectively). The Y-axis indicates the *P* values, while the X-axis specifies the fold change with respect to the control. The dashed line represents the limit between the significant cytokines (red), which are those with a *P* value less than 0.05, and those non-significant. As shown, GO exposure shows 31 cytokines significantly deregulated, most of them overexpressed-only PDGF-AA and PDGF-BB (platelet-derived growth factors) are under-expressed-, the most expressed being IL-6, CXCL1, CCL20, TNFA, and CCL3. Regarding GNPs exposure, the figure indicates 29 cytokines significantly deregulated. Interestingly, those overexpressed are shared with GO, and those under-expressed are PF4 and PDGF-BB. Finally, GNRs exposure shows 33 significant cytokines, also sharing with the other two GBN those that are overexpressed, except IL-6. Moreover, the under-expressed cytokines are ANG, APOA1, and RBP4. Supplementary Fig. 1 depicts the 51 cytokines that were significantly deregulated after LPS exposure (positive control).

Fig. 3 shows all those cytokines showing significant changes of expression, highlighting the existing interactions among them. The color of the nodules represents the functions in which they are involved,

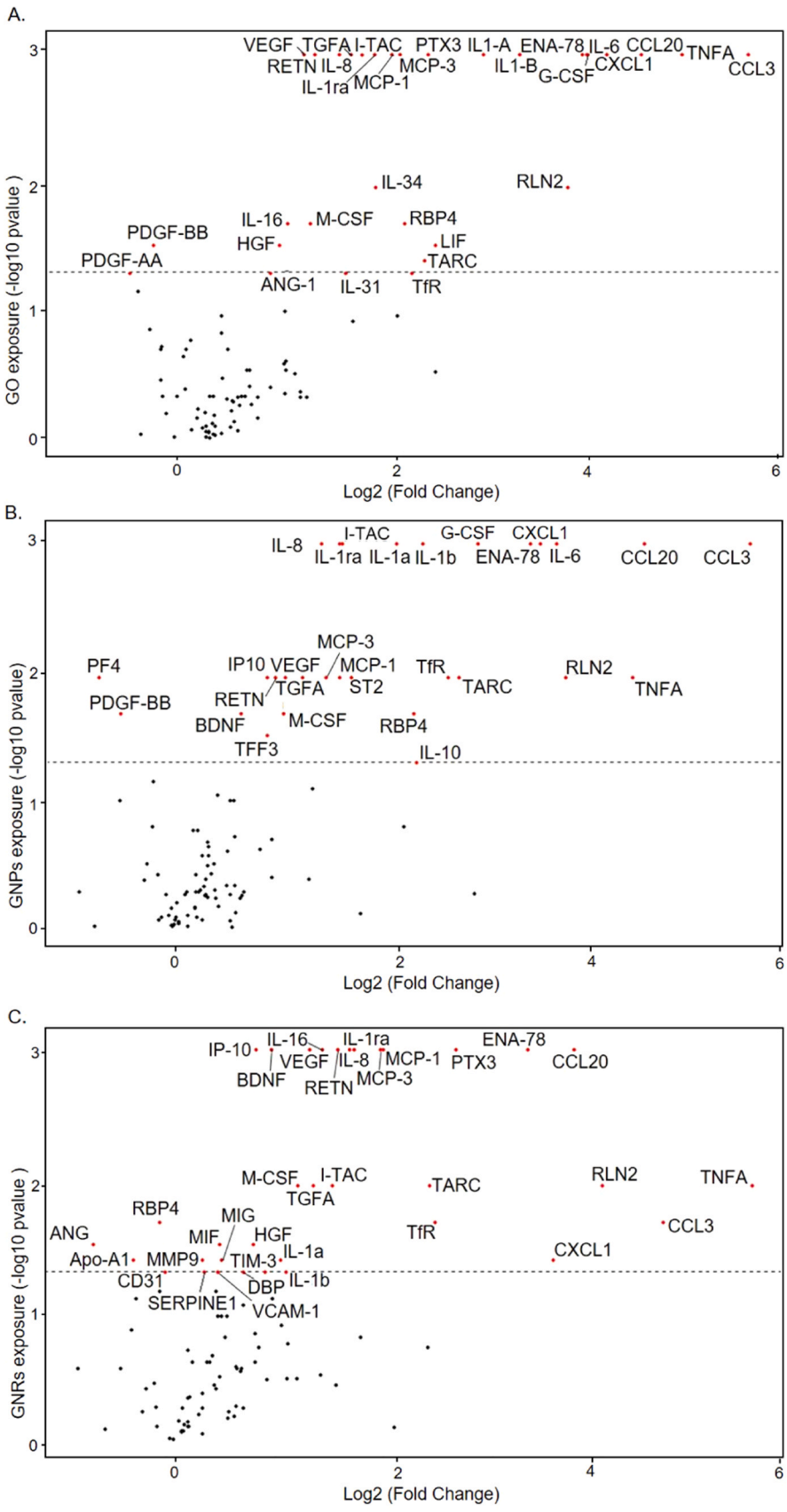

Fig. 2. Cytokine expression analysis after GBN exposure. Volcano Plot of secreted cytokines after the exposure to 50 μg/mL of GO (A), GNPs (B), GNRs (C). Each volcano plot is divided into two areas, the area above the dashed line represents the significant cytokines (in red) and the lower area depict the non-significant cytokines (in black). X axis depicts the log2 (Fold Change) and Y axis represents the –log10 (*P* value). Significance was calculated comparing cytokines expression from exposed samples to non-exposed ones by *t*-test (in red *P*-value < 0.05). The experiment was done with blood from 8 different donors. (For interpretation of the references to color in this figure legend, the reader is referred to the web version of this article.)

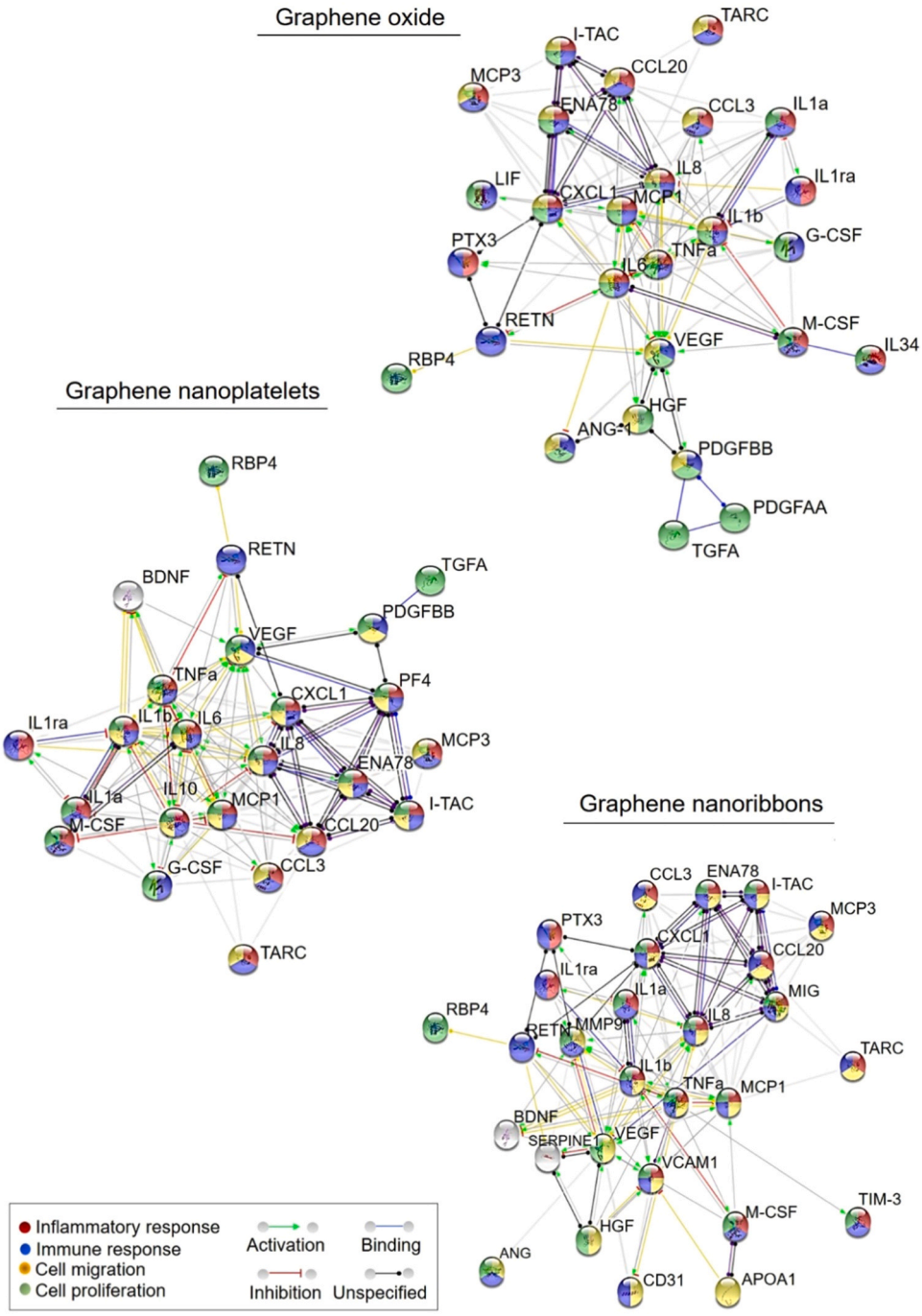

Fig. 3. STRING cytokine analysis of significantly dysregulated cytokines after GBN exposure Node colors represent functions in which they are implicated, and the networks express the different cytokines interactions. String Database Version 10.0 was used to generate the functional cytokines association networks. (For interpretation of the references to color in this figure legend, the reader is referred to the web version of this article.)

grouped in the inflammatory and the immune response, as well as cell migration, and proliferation. Some cytokines are category-specific, for example, TGFA, PDGFA or PF4 only participate in cell proliferation, RETN only participates in the immune response, and APOA1 only participates in cell migration. Instead, other cytokines have a role in all shown categories, like ENA-78, CCL2, IL1B, IL6 or TNF. It must be noted that although the expression of ST2, TFF3, IL-31, RLN2, IL-16, TFR, MIF, TGFA, and DBP is statistically significant, they do not appear in the STRING because they do not present interactions with other cytokines.

The cytokine expression patterns after the three GBN exposures were depicted at the Venn diagram (Fig. 4A). Some cytokines are exposure-specific while overlapping areas show the commonly expressed ones. Among them, Fig. 4B represents those cytokines which participate in the inflammatory response, being classified as pro-inflammatory cytokines and anti-inflammatory cytokines; and Fig. 4C highlights the most overexpressed cytokines after GO, GNPs, and GNRs exposures, showing CCL3 the highest increase. Instead, Fig. 5 displays the specific cytokines founded dysregulated after each GBN exposure. IL-34, LIF, PDGF-AA, ANG-1, and IL-31 are produced only by GO exposure whereas PF4, ST2, TFF3, and IL-10 are specifically produced by GNPs exposure. Finally, 8 cytokines were found dysregulated exclusively after GNRs exposure. Among them, MMP-9, MIF, S EPINE1, MIG, and VCAM-1 stand overexpressed compared to the non-exposed samples, while ANG, APOA1, and CD31 are under-expressed.

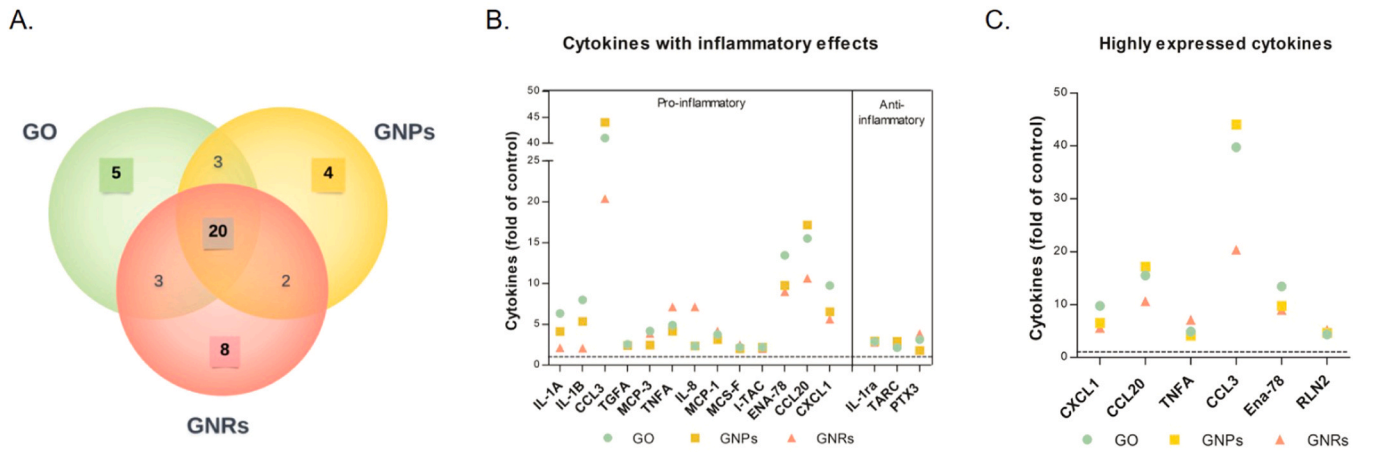

Fig. 4. (A) Venn Diagram shows the number of cytokines significantly dysregulated after treatment with each GBN. The overlapping area indicates the number of cytokines commonly dysregulated between the three GBN. (B) Analysis of selected cytokines with important effects on the inflammatory response. Cytokines are classified as pro-inflammatory or anti-inflammatory cytokines. (C) Highly expressed cytokines in all GBN exposures. Those cytokines overexpressed more than 4-folds over the control were considered. Data represent the folds of overexpression of the cytokines expressed in 8 different GBN-exposed samples compared to the non-exposed ones (controls). The dashed lines (B and C) represent the baseline expression of controls.

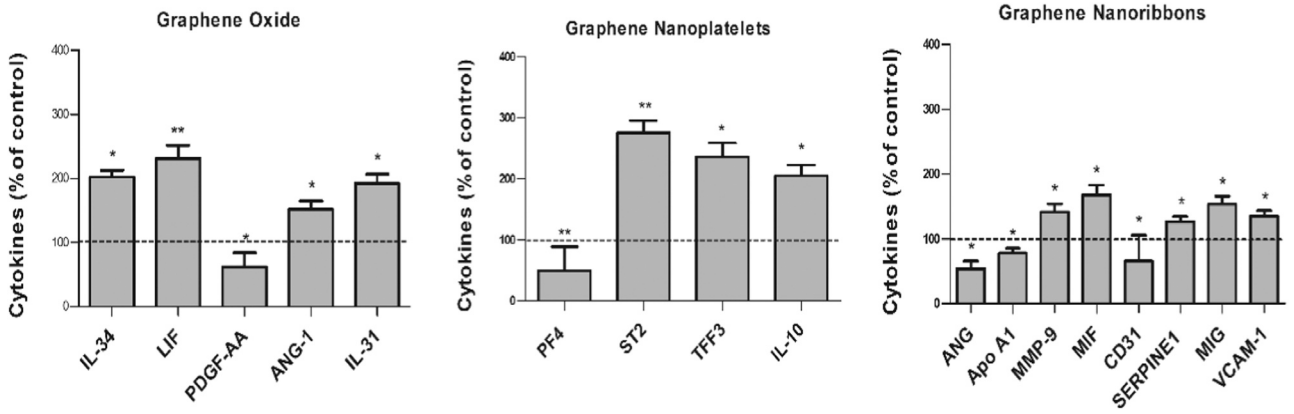

Fig. 5. Analysis of the cytokines over/under-expressed exclusively after the exposure to one of the GBNs analyzed. Controls are set as 100 (dashed lines represent the baseline expression of controls). *$P < 0.05$. **$P < 0.01$ (t-Student).

3.3. The soft-agar assay

The indirect soft-agar assay was performed to observe the functional effect of the secretome on cell growth ability. To measure this effect, HeLa cells (as a cell model) were exposed to serum (conditioned media) obtained from the blood previously treated with GBN. Fig. 6A shows representative images of the HeLa colonies growing under the different GBN exposures, as well as the negative and positive (LPS) controls. It can be appreciated an inhibitory effect on cells growing under the different treatments, but mainly with GO. Likewise, Fig. 6B represents the number of colonies growing with each GBN treatment. As observed in Fig. 6A, a high level of inhibition was observed with GO and GNPs and, although no in a marked way, GNRs were also able to inhibit cell growth. When the diameter of the colonies was evaluated, no significant differences for any GBN were detected except for GNPs where a low but significant ($P = 0.03$) effect was observed. The diameter of the colonies induced by LPS (positive control) was statistically significant regarding the negative control (Supplementary Fig. 2). As a summary, our results show an inhibitory effect on cell growth due to some of the components present in the secretome of whole blood cells after GBN exposure. It should be indicated that the potential remains of GBN in serum was not strictly checked but, instead, we made an indirect soft agar with HeLa cells exposed to DMEM treated with GBN (conditioned media). Additionally, this conditioned media was tested in HeLa cells without and after centrifugation. The results did not show any significant difference (P value > 0.05) in the number of colonies between the non-exposed samples and the GBN-exposed ones. Thus, we are confident that the observed effects are mainly due to the components of the secretome and not to the effect of the residual NPs that can be there.

4. Discussion

Due to the increasing use of GBN in biomedical applications, its potential impact on immune cells is a fundamental area requiring further responses. As previously indicated, applications like imaging or gene delivery make GBN to be in contact with the human immune system since the intravenous injection is one of the main routes of GBN administration. Several studies are proposing GO as a magnetic resonance imaging (MRI) contrast agent (Campbell et al., 2019), and GO-Fe_3O_4 nanoparticles have been proposed for optical cancer detection (Gonzalez-Rodriguez et al., 2019). In addition, to GO, other GBNs have also been proposed for such purposes. For instance, GNPs intercalated with manganese (Mn^{2+}) ions and functionalized with dextran (GNP-Dex) were proposed as a contrasting agent for clinical MRI (Kanakia et al., 2013). Furthermore, GNRs dispersed by carboxyphenylated substituent, and conjugated to aquated Gd^{3+} ions, have also been proposed as a high-performance contrast agent for applications in MRI (Gizzatov et al., 2014). In the present study, we have

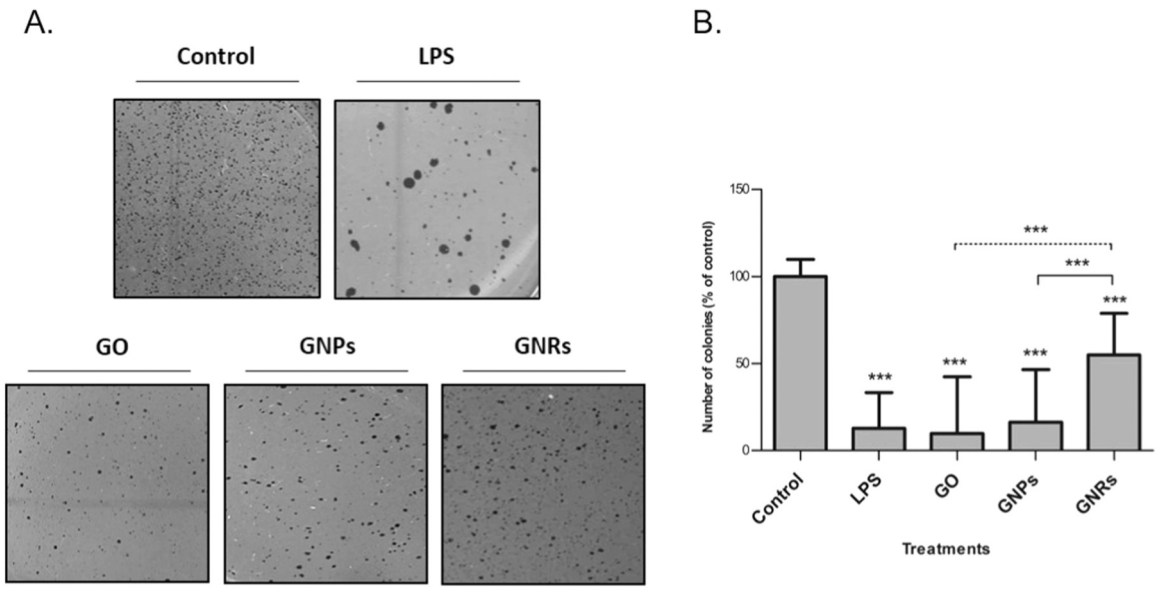

Fig. 6. Indirect soft-agar results of HeLa cells exposed to the serum extracted from blood samples previously treated with GO, GNPs, and GNRs. (A) Representative images corresponding to a section of the 35 mm soft-agar assay plates from each graphene. (B) Quantification of total colonies. Data represent mean ± SD-with controls set to 100%- of triplicates from 8 blood donors. ***$P < 0.001$ (t-Student).

proposed an *ex vivo* experimental model to unravel potential blood-nanomaterials interactions. It should be stated that in such context, our system could be a simple and sensitive method able to clarify the impact of GBN in the blood system by determining molecular changes at the secretome level. This could be a quick and easy way to determine biocompatibility between the different candidates with potential biomedical applicability. We have found that GBN exposure induces an immunological response, triggering important changes in the cytokine expression profile. This suggests that different sizes, forms, and physicochemical properties of GBN could impact human whole blood cells at the molecular level.

Studies evaluating the effects of GBN on the immune system using *in vivo* and *in vitro* approaches have reported controversial results (Dudek et al., 2016). For example, *in vitro* studies showed that GO could trigger IL-1β and TGF-β1 production in myeloid (THP-1) and epithelial (BEAS-2B) cells (Wang et al., 2015). Similarly, a caspase-dependent IL-1β expression in primary human monocyte-derived macrophages was observed after GO exposure (Mukherjee et al., 2018). Besides, although *in vitro* exposure to GO significantly increased the secretion of TNF-α by RAW-264.7 cells, no proinflammatory cytokine secretion was observed on primary immune cells (Feito et al., 2014). Furthermore, a recent study using an *in vitro* model of intestinal barrier showed a higher uptake of GNPs than GO, and both graphene compounds inducing low levels of anti-inflammatory cytokines, suggesting a weak anti-inflammatory response (Domenech et al., 2020).

Regarding *in vivo* studies, GO treatment significantly protected mice from α-GalCer-induced lethality proposing its use as an adjuvant in immunotherapy (Lee et al., 2018). In the same way, experiments *ex vivo* are controversial. Although it was reported that GO exposure caused significant changes in the lipid composition of the cell membrane of primary human neutrophils freshly isolated from healthy human blood donors (Mukherjee et al., 2018); small and large GO sheets were non-cytotoxic on peripheral blood mononuclear cells from healthy donors (Orecchioni et al., 2016).

By using our *ex vivo* exposure model, and using whole blood samples, we have detected that non-cytotoxic GBN exposure has an important impact on the whole blood secretome. It is important to remember that we have not follow the standard procedure of selecting candidate cytokines; our approach use a wide panel of cytokines what, at priory, has a higher chance of pick-up potential changes among the used set. Of the 105 analyzed cytokines, we have found that 19% are commonly deregulated in the three types of GBN. Among these proteins, most of them have pro-inflammatory effects, such as IL1α, IL1β, CCL3, TGFα(A), MCP3, TNFα, IL8,MCP1, MCSF, ITAC, ENA-78, CCL20, CXCL1, while others have anti-inflammatory effects, such as IL-1ra, TARC, PTX3. We would like to highlight the overexpression of TGFα and CXCL1, and, TNFα, IL-1 (α, or β). In the first case, TGFα is a protein described as the most prevalent and abundant in transformed cells and tumors. Together with CXCL1, they appear overexpressed in non-small cell lung cancer (Liu et al., 2017). On the other hand, different cytokines have been related to inflammatory processes. TNFα and IL-1 (α, or β) are among the most studied inflammatory cytokines in the tumor microenvironment (Balkwill and Mantovani, 2012). TNFα has a key role in inflammation and its overexpression has been related to many inflammatory diseases, like rheumatoid arthritis, ankylosing spondylitis, inflammatory bowel disease and psoriasis (Kany et al., 2019). In addition, it is worth to highlight that CCL3 is the most overexpressed cytokine of our study. CCL3 is an important inflammatory chemokine produced by a variety of cells, including macrophages. It participates as a potent activator of both innate and adaptive responses. Specifically, CCL3 plays an important role in the development, regulation and recruitment of leukocytes. Previous studies of our group corroborate CCL3 overexpression after the exposure to nanopolysytrene nanoparticles (Ballesteros et al., 2020). Similarly, other nanomaterials, like cooper or silver nanoparticles, induce an inflammatory response where CCL3 levels are significantly increased (Tang et al., 2019; Seiffert et al., 2016).

Alternatively, both GO and GNPs induce secretion of IL-6, G-CSF, and PDGF-BB. In the case of IL-6, it is a very well-studied pro-inflammatory cytokine. It has been considered as a key in tumorigenesis and metastasis processes since it is up-regulated in many types of cancers, including skin, breast, lung, esophageal, liver, pancreatic, gastric, colorectal, gynecological, prostate, kidney, bladder and hematological cancers as well as melanoma (Uciechowski and Dempke, 2020). Interestingly, and corroborating what we can observe in our study, IL-6, TNF-α, and G-CSF are a part of the inflammatory response triggered by GBN exposure. As in our study, an increase in the expression of IL-6, TNF-α, and G-CSF was observed in tissues surrounding an implant using graphene materials (Guazzo et al., 2018).

Since the majority of the altered cytokines observed in our study play a role in the immune response and are secreted by monocytes/

macrophages (da Cunha et al., 2019), we can consider these cells as the most implicated in the response to GBN exposure. This would agree with the results showing that GO induced the production of TNF-α in macrophages at the same levels that those induced by LPS exposure (Zhou et al., 2012). These results agree with those showing that pristine graphene and GO causes an increased production cytokines IL-1α, IL-6, IL-10, and TNFα by activated macrophages (Chen et al., 2012).

If we focus on those cytokines exclusively altered in response to one specific GBN, most of them are related to diseases associated with macrophage stimulation and inflammatory effects. For instance, if we focus on cytokines that appeared deregulated in GO exposure, we found that the overexpression of angiopoietin-1 (ANG-1) correlated to parameters of inflammation and bone destruction in inflammatory arthritis (Clavel et al., 2007); and IL-34 and IL-31 presenting an aberrant overexpression in Inflammatory Bowel Diseases (Zwicker et al., 2015). Similar occurs when we focus on the cytokines altered in GNPs exposure, we see that IL-10 stimulates the increased production of pro-inflammatory cytokines in atherosclerotic lesions (Mannino et al., 2015); while ST2 overexpression has been correlated with Inflammatory Bowel Disease (Boga et al., 2016). In the same line, if we observe those cytokines altered in GNRs, MIF is related with TNFα and IL6 key cytokines in cancer-related inflammation (Kulbe et al., 2012); VCAM-1 increased expression (vascular cell adhesion molecule-1) is closely associated with the progression of various immunological disorders, including rheumatoid arthritis, asthma, transplant rejection, and cancer (Kong et al., 2018). Analyzing the different proteins deregulated with the different types of GBN we cannot infer that one type of GBN is less biocompatible than another; we can only assume an equivalent risk for all of them, according to our results. Maybe the exception is GNRs exposure that triggers the overexpression of MMP9, a protein involved in the onset of cancer with important implications in the development of angiogenesis and inflammation, and with an indirect impact on the evolution of lung cancer (Rivas-Fuentes et al., 2015). Therefore, special attention should be paid to the effects induced by GNRs in future studies. In the same way, the comparison of *ex vivo* and *in vivo* data would help to confirm the goodness of the *ex vivo* approaches.

Besides the *ex vivo* system, another important feature of this study is the evaluation of the anchorage-independent growth to unravel the functional impact of the secretome. The secretome combines all the cytokine expression changes and the consequent changes of cytokines' interactions. Thus, any change in the anchorage-independent growth is reflecting the potential effects of the altered secretome on neighboring blood cells. Indeed, we are showing here that changes in the secretome produced by GBN can have an impact on the growth behavior of a model cell line. Although the transforming potential of carbon nanotubes compounds have been reported after chronic exposures (He et al., 2016; Vales et al., 2016) modulating the ability of anchorage-independent growth, as well as other hallmark biomarkers of cell transformation, no data using graphene-based materials have been found in the open literature. In this context, our results, showing that blood cells exposed to GBN are able to secrete compounds, look interesting and would need further studies to be demonstrated.

One of the limitations of the study is that we have not assess the role of concentration, or the effects associated to different sizes. Some studies like the one of Rodrigues et al. (2020), pointed out the importance of considering the size impact of graphene oxide nanomaterial (Rodrigues et al., 2020). In this sense, we consider that the study of these effects in further works will provide relevant information. Additionally, it should be mentioned that it is important to evaluate graphene effects at the level of WBCs subpopulations, since studies of our group have shown interesting results in that sense. Thus, the studies of Rubio et al. (2020) and Ballesteros et al. (2020) demonstrated that nanopolystyrene nanoparticles triggered differential biological effects both in different human hematopoietic cell lines and in blood cells analyzed in an *ex vivo* model such as the used in the present study. Likewise, Ballesteros et al. (2020) evidenced that the role of the concentrations must be considered as they found important differences in the cytokine's response due to the dose of nanoparticles. Furthermore, Orecchioni et al. (2017) demonstrated a different cytokine expression pattern depending on the immune cell population and the type of graphene oxide analyzed. Thus, rather than the complexity, future studies must focus in analyzing different sizes and concentrations of graphene nanomaterials, as well as evaluating their effects on WBCs.

As a conclusion, from our *ex vivo* model we have demonstrated that the selected GBN can trigger an immunological response that must be seriously evaluated when directly intravenously applied to humans. Besides, we propose that the *ex vivo* exposure used in this study can be useful to unravel potential health risks associated with GBN exposures.

CRediT authorship contribution statement

RM and AH planned the experiments. **SB and JD** carried out the experimental part. **SB and AV** analyzed the data, carried out the statistical analysis, and prepared tables/figures. **SB, RM, and AH** wrote the final manuscript.

Declaration of Competing Interest

The authors declare they have no actual or potential competing financial interests.

Acknowledgments

We wish to thank Mr. C. Valiente for his technical assistance. This work was partially supported by the Spanish Ministry of Education and Science [BFU2016-76831-R]. Sandra Ballesteros holds a fellowship from Universitat Autònoma de Barcelona [PIF-UAB].

Appendix A. Supporting information

Supplementary data associated with this article can be found in the online version at doi:10.1016/j.jhazmat.2021.125471.

References

Annangi, B., Bach, J., Vales, G., Rubio, L., Marcos, R., Hernández, A., 2015. Long-term exposures to low doses of cobalt nanoparticles induce cell transformation enhanced by oxidative damage. Nanotoxicology 9, 138–147. https://doi.org/10.3109/17435390.2014.900582.

Balkwill, F.R., Mantovani, A., 2012. Cancer-related inflammation: common themes and therapeutic opportunities. Semin. Cancer Biol. 22, 33–40. https://doi.org/10.1016/j.semcancer.2011.12.005.

Ballesteros, S., Domenech, J., Barguilla, I., Cortés, C., Marcos, R., Hernández, A., 2020. Genotoxic and immunomodulatory effects in human white blood cells after ex vivo exposure to polystyrene nanoplastics. Environ. Sci. Nano. https://doi.org/10.1039/D0EN00748J.

Boga, S., Alkim, H., Koksal, A.R., Ozagari, A.A., Bayram, M., Tekin Neijmann, S., Alkim, C., 2016. Serum ST2 in inflammatory bowel disease: a potential biomarker for disease activity. J. Investig. Med. 64, 1016–1024. https://doi.org/10.1136/jim-2016-000062.

Boraschi, D., Swartzwelter, B.J., Italiani, P., 2018. Interaction of engineered nanomaterials with the immune system: health-related safety and possible benefits. Curr. Opin. Toxicol. 10, 74–83. https://doi.org/10.1016/j.cotox.2018.02.002.

Campbell, E., Hasan, M.T., Pho, C., Callaghan, K., Akkaraju, G.R., Naumov, A.V., 2019. Graphene oxide as a multifunctional platform for intracellular delivery, imaging, and cancer sensing. Sci. Rep. 9, 416. https://doi.org/10.1038/s41598-018-36617-4.

Carpentier, G., 2009. ⟨http://image.bio.methods.free.fr/ImageJ/?Developpement-d-outils-d-analyse-et-de-traitement-d-images-avec-le-logiciel⟩.

Chen, G.-Y., Yang, H.-J., Lu, C.-H., Chao, Y.-C., Hwang, S.-M., Chen, C.-L., Lo, K.W., Sung, L.Y., Luo, W.Y., Tuan, H.Y., Hu, Y.-C., 2012. Simultaneous induction of autophagy and toll-like receptor signaling pathways by graphene oxide. Biomaterials 33, 6559–6569. https://doi.org/10.1016/j.biomaterials.2012.05.064.

Clavel, G., Bessis, N., Lemeiter, D., Fardellone, P., Mejjad, O., Ménard, J.F., Pouplin, S., Boumier, P., Vittecoq, O., Le Loët, X., Boissier, M.C., 2007. Angiogenesis markers (VEGF, soluble receptor of VEGF and angiopoietin-1) in very early arthritis and their association with inflammation and joint destruction. J. Clin. Immunol. 124, 158–164. https://doi.org/10.1016/j.clim.2007.04.014.

Cui, J., De Rose, R., Alt, K., Alcantara, S., Paterson, B.M., Liang, K., Hu, M., Richardson, J.J., Yan, Y., Jeffery, C.M., Price, R.I., Peter, K., Hagemeyer, C.E., Donnelly, P.S., Kent, S.J., Caruso, F., 2015. Engineering poly(ethylene glycol)

particles for improved biodistribution. ACS Nano 9, 1571–1580. https://doi.org/10.1021/nn5061578.
da Cunha, B.R., Domingos, C., Stefanini, A.C.B., Henrique, T., Polachini, G.M., Castelo-Branco, P., Tajara, E.H., 2019. Cellular interactions in the tumor microenvironment: the role of secretome. J. Cancer 10, 4574–4587. https://doi.org/10.7150/jca.21780.
Domenech, J., Hernández, A., Marcos, R., Cortés, C., 2020. Interactions of graphene oxide and graphene nanoplatelets with the *in vitro* Caco-2/HT29 model of intestinal barrier. Sci. Rep. 10, 2793. https://doi.org/10.1038/s41598-020-59755-0.
Dudek, I., Skoda, M., Jarosz, A., Szukiewicz, D., 2016. The molecular influence of graphene and graphene oxide on the immune system under *in vitro* and *in vivo* conditions. Arch. Immunol. Ther. Exp. 64, 195–215. https://doi.org/10.1007/s00005-015-0369-3.
Fadeel, B., 2019. Hide and seek: nanomaterial interactions with the immune system. Front. Immunol. 10, 133. https://doi.org/10.3389/fimmu.2019.00133.
Feito, M.J., Vila, M., Matesanz, M.C., Linares, J., Gonçalves, G., Marques, P.A., Vallet-Regí, M., Rojo, J.M., Portolés, M.T., 2014. In vitro evaluation of graphene oxide nanosheets on immune function. J. Colloid Interface Sci. 432, 221–228. https://doi.org/10.1016/j.jcis.2014.07.004.
Gizzatov, A., Keshishian, V., Guven, A., Dimiev, A.M., Qu, F., Muthupillai, R., Decuzzi, P., Bryant, R.G., Tour, J.M., Wilson, L.J., 2014. Enhanced MRI relaxivity of aquated Gd^{3+} ions by carboxyphenylated water-dispersed graphene nanoribbons. Nanoscale 6, 3059–3063. https://doi.org/10.1039/c3nr06026h.
Gonzalez-Rodriguez, R., Campbell, E., Naumov, A., 2019. Multifunctional graphene oxide/iron oxide nanoparticles for magnetic targeted drug delivery dual magnetic resonance/fluorescence imaging and cancer sensing. PLoS One 14, e0217072. https://doi.org/10.1371/journal.pone.0217072.
Guazzo, R., Gardin, C., Bellin, G., Sbricoli, L., Ferroni, L., Ludovichetti, F.S., Piattelli, A., Antoniac, I., Bressan, E., Zavan, B., 2018. Graphene-based nanomaterials for tissue engineering in the dental field. Nanomaterials 8, 349. https://doi.org/10.3390/nano8050349.
Han, S., Sun, J., He, S., Tang, M., Chai, R., 2019. The application of graphene-based biomaterials in biomedicine. Am. J. Transl. Res. 11, 3246–3260.
He, X., Despeaux, E., Stueckle, T.A., Chi, A., Castranova, V., Dinu, C.Z., Wang, L., Rojanasakul, Y., 2016. Role of mesothelin in carbon nanotube-induced carcinogenic transformation of human bronchial epithelial cells. Am. J. Physiol. Lung Cell. Mol. Physiol. 311, L538–L549. https://doi.org/10.1152/ajplung.00139.2016.
Iavicoli, I., Fontana, L., Leso, V., Corbi, M., Marinaccio, A., Leopold, K., Schindl, R., Lucchetti, D., Calapà, F., Sgambato, A., 2018. Subchronic exposure to palladium nanoparticles affects serum levels of cytokines in female Wistar rats. Hum. Exp. Toxicol. 37, 309–320. https://doi.org/10.1177/0960327117702952.
Kanakia, S., Toussaint, J.D., Chowdhury, S.M., Lalwani, G., Tembulkar, T., Button, T., Shroyer, K.R., Moore, W., Sitharaman, B., 2013. Physicochemical characterization of a novel graphene-based magnetic resonance imaging contrast agent. Int. J. Nanomed. 8, 2821–2833. https://doi.org/10.2147/IJN.S47062.
Kany, S., Vollrath, J.T., Relja, B., 2019. Cytokines in inflammatory disease. Int. J. Mol. Sci. 20, 6008. https://doi.org/10.3390/ijms20236008.
Kong, D.H., Kim, Y.K., Kim, M.R., Jang, J.H., Lee, S., 2018. Emerging roles of vascular cell adhesion molecule-1 (VCAM-1) in immunological disorders and cancer. Int. J. Mol. Sci. 19, 1057. https://doi.org/10.3390/ijms19041057.
Kulbe, H., Chakravarty, P., Leinster, D.A., Charles, K.A., Kwong, J., Thompson, R.G., Coward, J.I., Schioppa, T., Robinson, S.C., Gallagher, W.M., Galletta, L., Australian Ovarian Cancer Study Group, Salako, M.A., Smyth, J.F., Hagemann, T., Brennan, D. J., Bowtell, D.D., Balkwill, F.R., 2012. A dynamic inflammatory cytokine network in the human ovarian cancer microenvironment. Cancer Res. 72, 66–75. https://doi.org/10.1158/0008-5472.CAN-11-2178.
Lee, S.W., Park, H.J., Van Kaer, L., Hong, S., Hong, S., 2018. Graphene oxide polarizes iNKT cells for production of TGFβ and attenuates inflammation in an iNKT cell-mediated sepsis model. Sci. Rep. 8, 10081. https://doi.org/10.1038/s41598-018-28396-9.
Lin, J., Chen, X., Huang, P., 2016. Graphene-based nanomaterials for bioimaging. Adv. Drug Deliv. Rev. 105, 242–254. https://doi.org/10.1016/j.addr.2016.05.013.
Liu, X., Chen, L., Tian, X.D., Zhang, T., 2017. MiR-137 and its target TGFA modulate cell growth and tumorigenesis of non-small cell lung cancer. Eur. Rev. Med. Pharmacol. Sci. 21, 511–517.
Loh, K.P., Ho, D., Chiu, G.N.C., Leong, D.T., Pastorin, G., Chow, E.K., 2018. Clinical applications of carbon nanomaterials in diagnostics and therapy. Adv. Mater. 30, 1802368 https://doi.org/10.1002/adma.201802368.
Madannejad, R., Shoaie, N., Jahanpeyma, F., Darvishi, M.H., Azimzadeh, M., Javadi, H., 2019. Toxicity of carbon-based nanomaterials: reviewing recent reports in medical and biological systems. Chem. Biol. Interact. 307, 206–222. https://doi.org/10.1016/j.cbi.2019.04.036.
Mann, S.K., Dufour, A., Glass, J.J., De Rose, R., Kent, S.J., Such, G.K., Johnston, A.P.R., 2016. Tuning the properties of pH responsive nanoparticles to control cellular interactions: in vitro and ex vivo. Polym. Chem. 7, 6015–6024. https://doi.org/10.1039/c6py01332e.
Mannino, M.H., Zhu, Z., Xiao, H., Bai, Q., Wakefield, M.R., Fang, Y., 2015. The paradoxical role of IL-10 in immunity and cancer. Cancer Lett. 367, 103–107. https://doi.org/10.1016/j.canlet.2015.07.009.
Mukherjee, S.P., Kostarelos, K., Fadeel, B., 2018. Cytokine profiling of primary human macrophages exposed to endotoxin-free graphene oxide: size-independent nlrp3 inflammasome activation. Adv. Healthc. Mater. 7, 1700815 https://doi.org/10.1002/adhm.201700815.
Nanogenotox, 2011. (http://www.nanogenotox.eu/files/PDF/Deliverables/nanogenotox%20deliverable%203wp4%20dispersion%20protocol.pdf).
Orecchioni, M., Jasim, D.A., Pescatori, M., Manetti, R., Fozza, C., Sgarrella, F., Bedognetti, D., Bianco, A., Kostarelos, K., Delogu, L.G., 2016. Molecular and genomic impact of large and small lateral dimension graphene oxide sheets on human immune cells from healthy donors. Adv. Healthc. Mater. 5, 276–287. https://doi.org/10.1002/adhm.201500606.
Orecchioni, M., Bedognetti, D., Newman, L., Fuoco, C., Spada, F., Hendrickx, W., Marincola, F.M., Sgarrella, F., Rodrigues, A.F., Ménard-Moyon, C., Cesareni, G., Kostarelos, K., Bianco, A., Delogu, L., 2017. Single-cell mass cytometry and transcriptome profiling reveal the impact of graphene on human immune cells. Nat. Commun. 8, 1109. https://doi.org/10.1038/s41467-017-01015-3.
Park, E.J., Kim, S.N., Kang, M.S., Lee, B.S., Yoon, C., Jeong, U., Kim, Y., Lee, G.H., Kim, D.W., Kim, J.S., 2016. A higher aspect ratio enhanced bioaccumulation and altered immune responses due to intravenously-injected aluminum oxide nanoparticles. J. Immunotoxicol. 13, 439–448. https://doi.org/10.3109/1547691X.2015.1122116.
Patel, S., Ngounou Wetie, A.G., Darie, C.C., Clarkson, B.D., 2014. Cancer secretomes and their place in supplementing other hallmarks of cancer. Adv. Exp. Med. Biol. 806, 409–442. https://doi.org/10.1007/978-3-319-06068-2_20.
Ramos, A.P., Cruz, M.A.E., Tovani, C.B., Ciancaglini, P., 2017. Biomedical applications of nanotechnology. Biophys. Rev. 9, 79–89. https://doi.org/10.1007/s12551-016-0246-2.
Rivas-Fuentes, S., Salgado-Aguayo, A., Pertuz Belloso, S., Gorocica Rosete, P., Alvarado-Vásquez, N., Aquino-Jarquin, G., 2015. Role of chemokines in non-small cell lung cancer: angiogenesis and inflammation. J. Cancer 6, 938–952. https://doi.org/10.7150/jca.12286.
Rodrigues, A.F., Newman, L., Jasim, D., Mukherjee, S.P., Wang, J., Vacchi, I.A., Bussy, C., 2020. Size-dependent pulmonary impact of thin graphene oxide sheets in mice: toward safe-by-design. Adv. Sci. 7, 1903200 https://doi.org/10.1002/advs.201903200.
Rubio, L., Barguilla, I., Domenech, J., Marcos, R., Hernández, A., 2020. Biological effects, including oxidative stress and genotoxic damage, of polystyrene nanoparticles in different human hematopoietic cell lines. J. Hazard. Mater. 398, 122900 https://doi.org/10.1016/j.jhazmat.2020.122900.
Seiffert, J., Buckley, A., Leo, B., Martin, N.G., Zhu, J., Dai, R., Hussain, F., Guo, C., Warren, J., Hodgson, A., Gong, J., Ryan, M.P., Zhang, J.J., Porter, A., Tetley, T.D., Gow, A., Smith, R., Chung, K.F., 2016. Pulmonary effects of inhalation of spark-generated silver nanoparticles in Brown-Norway and Sprague–Dawley rats. Respir. Res. 17, 85. https://doi.org/10.1186/s12931-016-0407-7.
Song, S., Shen, H., Wang, Y., Chu, X., Xie, J., Zhou, N., Shen, J., 2020. Biomedical application of graphene: from drug delivery, tumor therapy, to theranostics. Colloids Surf. B Biointerfaces 185, 110596. https://doi.org/10.1016/j.colsurfb.2019.110596.
Szklarczyk, D., Franceschini, A., Wyder, S., Forslund, K., Heller, D., Huerta-Cepas, J.C., 2015. STRING v10: protein-protein interaction networks, integrated over the tree of life. Nucleic Acids Res. 43, D447–D452. https://doi.org/10.1093/nar/gku1003.
Tang, H., Xu, M., Luo, J., Zhao, L., Ye, G., Shi, F., Ménard-Moyon, C., Bianco, A., Fadeel, B., Kostarelos, K., Li, Y., 2019. Liver toxicity assessments in rats following sub-chronic oral exposure to copper nanoparticles. Environ. Sci. Eur. 31, 30. https://doi.org/10.1186/s12302-019-0214-0.
Uciechowski, P., Dempke, W.C.M., 2020. Interleukin-6: a masterplayer in the cytokine network. Oncology 98, 131–137. https://doi.org/10.1159/000505099.
Vales, G., Rubio, L., Marcos, R., 2016. Genotoxic and cell-transformation effects of multi-walled carbon nanotubes (MWCNT) following in vitro sub-chronic exposures. J. Hazard. Mater. 306, 193–202. https://doi.org/10.1016/j.jhazmat.2015.12.021.
Vila, L., Marcos, R., Hernández, A., 2017. Long-term effects of silver nanoparticles in Caco-2 cells. Nanotoxicology 11, 771–780. https://doi.org/10.1080/17435390.2017.1355997.
Wang, X., Duch, M.C., Mansukhani, N., Ji, Z., Liao, Y.P., Wang, M., Zhang, H., Sun, B., Chang, C.H., Li, R., Lin, S., Meng, H., Xia, T., Hersam, M.C., Nel, A.E., 2015. Use of a pro-fibrogenic mechanism-based predictive toxicological approach for tiered testing and decision analysis of carbonaceous nanomaterials. ACS Nano 9, 3032–3043. https://doi.org/10.1021/nn507243w.
Zhou, H., Zhao, K., Li, W., Yang, N., Liu, Y., Chen, C., Wei, T., 2012. The interactions between pristine graphene and macrophages and the production of cytokines/chemokines via TLR- and NF-κB-related signaling pathways. Biomaterials 33, 6933–6942. https://doi.org/10.1016/j.biomaterials.2012.06.064.
Zwicker, S., Martinez, G.L., Bosma, M., Gerling, M., Clark, R., Majster, M., Söderman, J., Almer, S., Boström, E.A., 2015. Interleukin 34: a new modulator of human and experimental inflammatory bowel disease. Clin. Sci. 129, 281–290. https://doi.org/10.1042/CS20150176.